Local Base Dynamics and Local Structural Features in RNA and DNA Duplexes†

Shih-Chung Kao and Albert M. Bobst*
Department of Chemistry, University of Cincinnati, Cincinnati, Ohio 45221
Received December 14, 1984

ABSTRACT: Local base motion and local structural base information are derived with a simple motional model from site specifically spin-labeled polyribo- and polydeoxyribonucleotides. The model was developed earlier for some nucleic acids and has now been applied to analyze 22 different nucleic acid systems. We conclude that the base motion of the spin-labeled nucleotide in single-stranded RNA, DNA, or non-base-paired bases in duplexes is of the order of 1 ns and that its base mobility decreases by about a factor of 4 upon base pairing. Also, the tether motion of the probe is slower in an RNA than in a DNA duplex.

The study of nuclei acid conformation and flexibility is of importance for understanding the polymorphism found in nucleic acids. The conformational and dynamic aspects of nucleic acids have been studied by a variety of techniques (Bolton & James, 1979; Early & Kearns, 1979; Hogan & Jardetzky, 1979; Klevan et al., 1979; Bobst, 1980; Robinson et al., 1980a,b; Allison et al., 1982; Hurley et al., 1982; Keepers & James, 1982; Wang et al.; Saenger, 1984). Motions suggested from the Barkley–Zimm calculations involve substantial changes in the nucleic acid geometry in the time range from 1 to 100 ns (Barkley & Zimm, 1979). A number of NMR relaxation studies of various ^{1}H-, ^{13}C-, and ^{31}P-labeled nuclei in DNA[1] fragments of different sizes were published that lead to different conclusions regarding base motion. Recently, Assa-Munt et al. (1984) concluded that a good fit of their NMR data collected on 53 base-pair fragments of $(dA\text{-}dT)_n$ can be obtained by using a correlation time of 0.7 ns for internal motion and an angular displacement of 32° for the bases relative to the helix axis. We have had experimental evidence for base-dependent rapid motions in nucleic acids for many years (Bobst, 1971, 1972; Pan & Bobst, 1973; Bobst et al., 1981), but only more recently were we able to establish unequivocally with a simple motional model that the high-frequency local motions observed with spin-labeled nucleic acids are caused by rapid base motions (Kao et al., 1983; Bobst et al., 1984). We have been using ESR as a detection tool to detect these rapid motions, a technique ideally suited to measure motions occurring on a nanosecond time scale. The nucleic acids have been enzymatically spin-labeled with probes attached either in position 4 or in position 5 of ribo- and deoxyribonucleosides as shown in Figures 1 and 2, respectively. In the latter position, tethers of different length were used, which allowed us also to get some geometric information about the depth of the major groove in B-like DNA (Bobst et al., 1984). Preliminary results with the uvrABC protein complex have shown that a substitution in position 5 in the case of the spin-labeled duplex $(DUMPT,dT)_n{\cdot}(dA)_n$ (Bobst et al., 1984) causes no distortional sites in the duplex (Grossman, private communication), and it was shown earlier with thermal melting curves that a substitution in position 5 does not affect the T_m^{OD} of the duplex (Langemeier & Bobst, 1981).

In the present study, we reinforce our finding of fast localized internal motions of bases in RNA and DNA systems. This was achieved by expanding our previous set of spin-labeled nucleic acids and analyzing their ESR spectra with the same motional model used earlier. The model encompasses both individual base-pair motions and correlated bending and twisting motions as described by Barkley & Zimm (1979). It has allowed us to analyze all 22 spin-labeled nucleic acid systems so far synthesized. It is reassuring to note that this ESR approach, which requires the incorporation of strategically placed probes, gives results agreeing with the latest NMR interpretations in terms of local base mobility (Assa-Munt et al., 1984). The motional model used for the interpretation of ESR data of spin-labeled nucleic acids not only makes it possible to draw conclusions about the local dynamics of RNA and DNA systems but also gives some information about their structural characteristics.

Materials and Methods

$(A)_n$ and $(dA)_n$ were purchased from P-L Biochemicals and were purified through Sephacryl S-200 before use. The CPK precision molecular models were bought from the Ealing Corp. All other materials were commercial products of analytical reagent grade.

Enzymatic Synthesis of Spin-Labeled RNA. The chemical structures of the 5- and 4-substituted nitroxide-labeled ribonucleosides are given in Figure 1. $(ls^4U,U)_n$ was prepared according to a published procedure from this laboratory (Warwick et al., 1980). All other spin-labeled RNAs were prepared under conditions similar to those described for $(ls^4U,U)_n$ by copolymerizing uridine 5′-diphosphate and the appropriate nitroxide-containing nucleoside 5′-diphosphate analogues with polynucleotide phosphorylase. The synthesis of the diphosphate analogues ppRUMMT, ppRUTT, ppRUMPT, and $ppls^4U$ has been published (Kao et al., 1983),

† This investigation was supported in part by a grant from the U.S. Public Health Service (GM 27002).

[1] Abbreviations: $(A)_n$, poly(adenylic acid); $(U)_n$, poly(uridylic acid); $(dA)_n$, poly(deoxyadenylic acid); $(dT)_n$, poly(deoxythymidylic acid); $(RUMMT,U)_n$, copolymer of RUMMT and uridine; $(RUTT,U)_n$, copolymer of RUTT and uridine; $(RUMPT,U)_n$, copolymer of RUMPT and uridine; $(lss^4U,U)_n$, copolymer of lss^4U and uridine; $(ls^4U,U)_n$, copolymer of ls^4U and uridine; $(DUMMT,dT)_n$, copolymer of DUMMT and thymidine; $(DUTT,dT)_n$, copolymer of DUTT and thymidine; $(DUMPT,dT)_n$, copolymer of DUMPT and thymidine; $(DUMBT,dT)_n$, copolymer of DUMBT and thymidine; $(DUAT,dT)_n$, copolymer of DUAT and thymidine; $(ls^4dU,dT)_n$, copolymer of ls^4dU and thymidine; RNA, ribonucleic acid; DNA, deoxyribonucleic acid; $\tau_\parallel$ and $\tau_\perp$, correlation times for rotations about and perpendicular to the principal axis of diffusion, respectively; T_m^{OD}, melting temperature determined by UV spectroscopy; ESR, electron spin resonance. Structures of the abbreviated uridine analogues RUMMT, RUTT, RUMPT, lss^4U, and ls^4U are given in Figure 1 and those of the deoxyuridine analogues DUMMT, DUTT, DUMPT, DUMBT, DUAT, and ls^4dU in Figure 2.

0006-2960/85/0424-5465$01.50/0

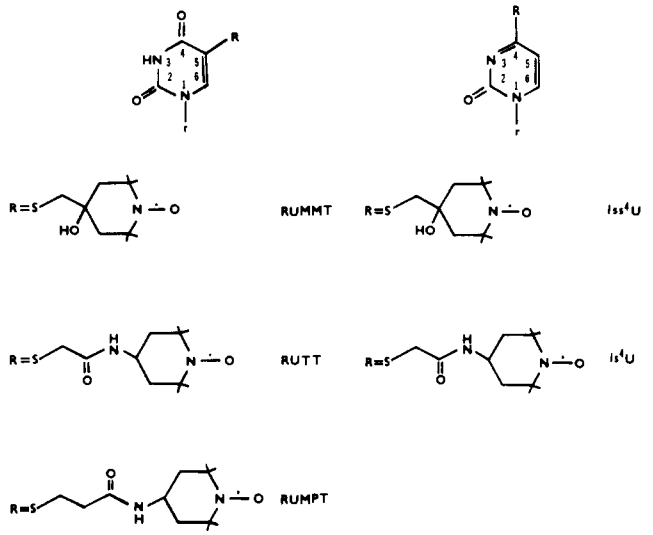

FIGURE 1: Chemical structure of 5- or 4-substituted spin-labeled uridine derivatives.

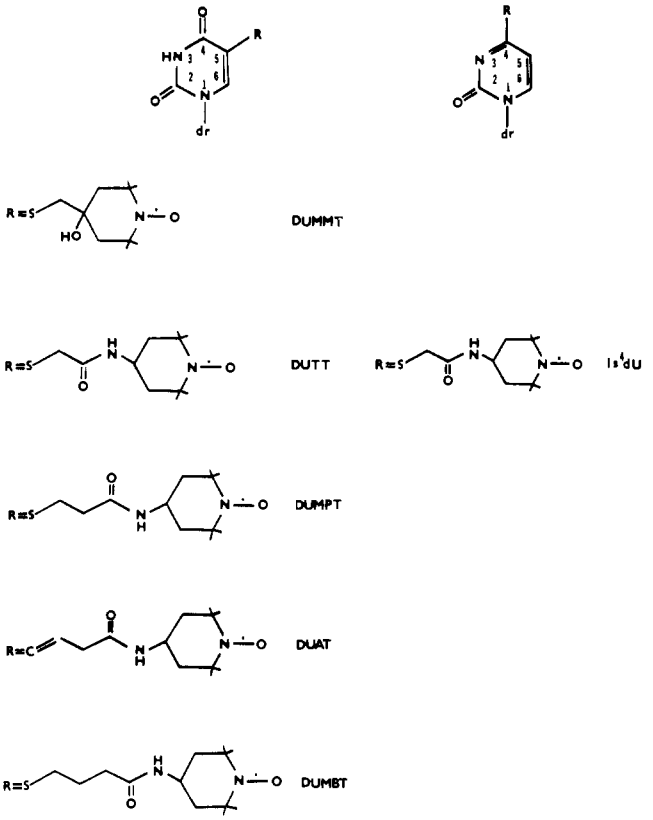

FIGURE 2: Chemical structure of 5- or 4-substituted spin-labeled deoxyuridine derivatives.

and the synthesis of pplss^{4}U will be published elsewhere (Toppin et al., 1985).

Enzymatic Synthesis of Spin-Labeled DNA. The chemical structures of the 5- and 4-substituted nitroxide-labeled deoxyribonucleosides are shown in Figure 2. $(DUTT,dT)_n$ was prepared according to a published procedure (Toppin et al., 1983). All other spin-labeled DNAs were prepared under conditions similar to those published for $(DUTT,dT)_n$ by copolymerizing thymidine 5′-triphosphate with the appropriate nitroxide-containing deoxynucleoside 5′-triphosphate analogues with terminal deoxynucleotidyl transferase. The synthesis of the triphosphate analogues pppDUMMT, pppDUTT, pppDUMPT, and pppDUMBT has been published (Bobst et al., 1984), and the synthesis of pppDUAT and ppls^{4}dU will be published elsewhere (Toppin et al., 1985).

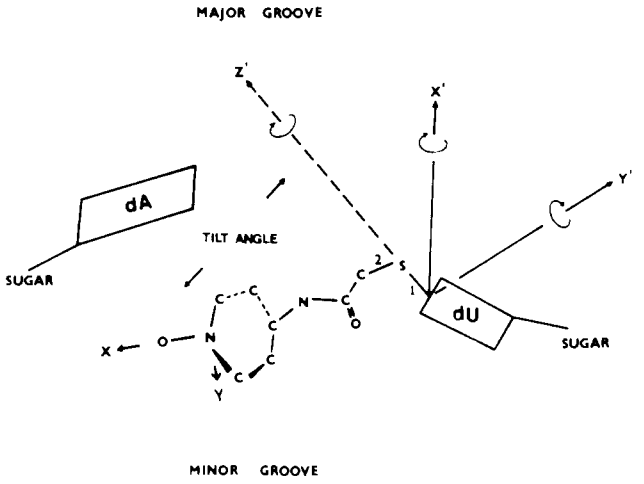

FIGURE 3: Schematic diagram of dA and non-base-paired ls^{4}dU. The molecular fixed hyperfine principal x axis is tilted by an angle with respect to the principal rotational diffusion axis z'.

Characterization of Spin-Labeled Nucleic Acids. All spin-labeled nucleic acids were characterized by gel electrophoresis to determine the lattice size and by enzymatic digestion to measure the nitroxide-labeled nucleotide to unmodified nucleotide ratio (Hakam et al., 1980; Toppin et al., 1983). The ones used for this study had a weight-average molecular weight of 100 000–200 000 and contained 1–2% of spin-labeled nucleotides.

ESR Measurements and Simulation of ESR Spectra. Ambient-temperature spectra of air-saturated samples were recorded at 100-G spectral width with a Varian E-104 spectrometer interfaced to an Apple II plus microcomputer (Ireland et al., 1983). The modulation amplitude was 1 G, and the microwave power was kept at 10 mW. The ESR simulations were carried out on an Amdahl 470 computer with a tilt program used by Polnaszek (1976). The simulation program takes into account anisotropic rotational motion and is characterized by two correlation times, $\tau_\parallel$ for motions about the principal axis of diffusion z' and $\tau_\perp$ for motions about the two orthogonal diffusion axes of the molecule. The line-broadening term T_2^{-1} (Freed, 1976), reflecting broadening by unresolved proton splittings and other interactions independent of motion, was determined by fitting the central line of the experimental spectra. The uncertainty in the τ values is of the order of 10%. The experimental and simulated spectra were plotted on an Houston Instrument DMP-3 digital plotter.

Results and Discussion

Some of the chemical structures of the 5- or 4-substituted nitroxide-labeled ribonucleosides and deoxyribonucleosides used to determine base mobilities have been reported earlier (Kao et al., 1983; Bobst et al., 1984). Among the new structures is DUAT (Figure 2), whose tether is similar in length to that of DUMPT (Figure 2) but has a double bond instead of a single bond next to the tether carbon–pyrimidine linkage. ls^{4}dU is the deoxyribose analogue of ls^{4}U and is also new. Finally, the tether length in ls^{4}U was shortened by one bond to give the novel compound lss^{4}U.

For the analysis of a total of 22 ESR spectra of spin-labeled single and double strands we can apply the same simple motional model as described earlier (Kao et al., 1983; Bobst et al., 1984). In this model [see Figure 5 in Bobst et al. (1984)], the principal rotational diffusion axis z' is defined along the tether pyrimidine linkage (see bond 1 in Figure 3) for both double- and single-stranded nucleic acids. With

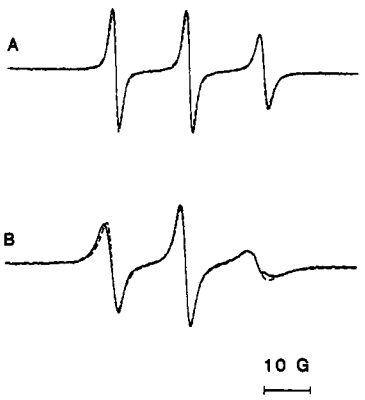

FIGURE 4: Experimental (—) and computer simulated (--) ESR spectra of (A) 0.9×10^{-4} M $(DUAT,dT)_n$ and (B) 1.9×10^{-4} M $(DUAT,dT)_n \cdot (dA)_n$. The experimental spectra were taken in 0.01 M NaCl–0.01 M sodium cacodylate (pH 7). The computer-simulated spectra were obtained as described under Materials and Methods with the parameters given in Tables I and II.

Figure 3 we also show the schematic diagram for ls^{4}dU, which is non base paired with dA. The principal rotational diffusion axis z' is defined as earlier along the tether pyrimidine linkage (bond 1). Note the position of bond 2 in the tether, which is the same for the non-base-paired system shown here as for the base-paired example given earlier [Figure 5 in Bobst et al. (1984)]. In the case of a duplex with a defined geometry such as B DNA, one of the axes of the correlation time $\tau_\perp$ is parallel to the helical axis. $\tau_\perp$ will reflect base motion arising from tilting and torsion of base pairs as well as twisting of bases, whereas $\tau_\parallel$ represents tether motion in the duplex. We found that the same motional model was applicable to single strands, since as in the duplex $\tau_\perp$ was found to be tether independent and $\tau_\parallel$ to be tether dependent. Thus, we assign for $\tau_\parallel$ and $\tau_\perp$ the same meaning for both single and double strands.

Experimental and computer-simulated ESR spectra of $(DUAT,dT)_n$ and $(DUAT,dT)_n \cdot (dA)_n$ are given in Figure 4. $(DUAT,dT)_n$ gives a narrow-lined spectrum characteristic of non-base-paired spin-labeled nucleotides, whereas $(DUAT,dT)_n \cdot (dA)_n$ shows a more broadened spectrum with a line shape usually observed for base-paired spin-labeled nucleotides. The simulations of the spectra shown in Figure 4 were achieved with the parameters given in Tables I and II. For comparative purposes the simulation parameters are also listed for DUMMT, DUTT, DUMPT, and DUMBT containing nucleic acids, which are all 5-substituted spin-labeled nucleic acid systems. Note that the tether lengths in DUAT and DUMPT are very similar (Figure 2) and the ESR spectra for both labels are essentially identical in single and double strands. This is also reflected in the parameter values used for the simulations (Tables I and II). These findings suggest that the presence of a double or a single bond at bond 2 does not affect the base mobility, further supporting the model, in which the fast axis of reorientation is along bond 1 of the tether and $\tau_\perp$ reflects indeed base motions.

Theory and mathematical models were recently developed by Keepers & James (1982) to elucidate the motions in double-stranded DNA on the basis of NMR relaxation properties. Internal rotation correlation times in the 0.3–0.6-ns range for phosphorus internal motion and in the 0.5–2.0-ns range for conformational fluctuations in the deoxyribose ring gave the best fit to the experimental NMR data. More resently, Assa-Munt et al. (1984) achieved a good fit of their NMR data with a three-state jump model for the localized internal motions of the base pairs and by using a correlation time for the internal motion of 0.7 ns and an angular displacement of the bases of ±32° relative to the helix axis. Our interpretation of the ESR data obtained on various site specifically spin-labeled nucleic acids led us to conclude that the base motion in nucleic acids occurs in the nanosecond time domain. It is interesting to note that the model used by Assa-Munt et al. (1984) to calculate base mobilities from NMR data gives correlation times that are consistent with

Table I: Motional Parameters of Probe in Single-Stranded RNA and DNA Systems[a]

single strands	$\tau_\parallel$ (ns)	$\tau_\perp$ (ns)	tilt angle (deg)	z' = fast axis of reorientation
RNA Systems				
probe in position 5				
$(RUMMT,U)_n$[b]	0.1	1.2	45 ± 5	$z' = z$
$(RUTT,U)_n$[b]	0.09	1.2	55 ± 5	$z' = z$
$(RUMPT,U)_n$[b]	0.08	1.2	55 ± 5	$z' = z$
probe in position 4				
$(lss^4U,U)_n$	0.1	1.2	45 ± 5	$z' = z$
$(ls^4U,U)_n$[b]	0.07	1.2	55 ± 5	$z' = z$
DNA Systems				
probe in position 5				
$(DUMMT,dT)_n$[c]	0.09	1.2	45 ± 5	$z' = z$
$(DUTT,dT)_n$[c]	0.07	1.2	55 ± 5	$z' = z$
$(DUMPT,dT)_n$[c]	0.06	1.2	55 ± 5	$z' = z$
$(DUAT,dT)_n$	0.06	1.2	55 ± 5	$z' = z$
$(DUMBT,dT)_n$[c]	0.03	1.2	55 ± 5	$z' = z$
probe in position 4				
$(ls^4dU,dT)_n$	0.05	1.2	50 ± 5	$z' = z$

[a] Nitroxide ESR parameters: A_{xx} = 7.15 G; A_{yy} = 7.35 G; A_{zz} = 35.6 G; g_{xx} = 2.0088; g_{yy} = 2.0059; g_{zz} = 2.0026. T_2^{-1} = 0.8 G for $(RUMMT,U)_n$, $(lss^4U,U)_n$, and $(DUMMT,dT)_n$ and 1.2 G for $(RUTT,U)_n$, $(RUMPT,U)_n$, $(ls^4U,U)_n$, $(DUTT,dT)_n$, $(DUMPT,dT)_n$, $(DUAT,dT)_n$, $(DUMBT,dT)_n$, and $(ls^4dU,dT)_n$. [b] From Kao et al. (1983). [c] From Bobst et al. (1984).

Table II: Motional Parameters of Probe in Double-Stranded RNA and DNA Systems[a]

double strands	$\tau_\parallel$ (ns)	$\tau_\perp$ (ns)	tilt angle (deg)	z' = fast axis of reorientation
RNA Systems				
probe in position 5				
$(RUMMT,U)_n \cdot (A)_n$[b]	2	4	80 ± 5	$z' = z$
$(RUTT,U)_n \cdot (A)_n$[b]	0.5	4	40 ± 5	$z' = z$
$(RUMPT,U)_n \cdot (A)_n$[b]	0.4	4	40 ± 5	$z' = z$
probe in position 4				
$(lss^4U,U)_n \cdot (A)_n$	0.7	2.8	80 ± 5	$z' = x$
$(ls^4U,U)_n \cdot (A)_n$	0.2	1.2	50 ± 5	$z' = x$
$(ls^4U,U)_n \cdot (A)_n$[b]	0.1	1.2	40 ± 5	$z' = z$
DNA Systems				
probe in position 5				
$(DUMMT,dT)_n \cdot (dA)_n$[c]	0.7	4	80 ± 5	$z' = x$
$(DUTT,dT)_n \cdot (dA)_n$[c]	0.3	4	40 ± 5	$z' = z$
$(DUMPT,dT)_n \cdot (dA)_n$[c]	0.2	4	40 ± 5	$z' = z$
$(DUAT,dT)_n \cdot (dA)_n$	0.2	4	40 ± 5	$z' = z$
$(DUMBT,dT)_n \cdot (dA)_n$[c]	0.06	4	55 ± 5	$z' = z$
probe in position 4				
$(ls^4dU,dT)_n \cdot (dA)_n$	0.05	1.2	55 ± 5	$z' = x$

[a] Nitroxide ESR parameters for $(RUTT,U)_n \cdot (A)_n$, $(RUMPT,U)_n \cdot (A)_n$, $(ls^4U,U)_n \cdot (A)_n$,[b] $(DUTT,dT)_n \cdot (dA)_n$, $(DUMPT,dT)_n \cdot (dA)_n$, $(DUAT,dT)_n \cdot (dA)_n$, and $(DUMBT,dT)_n \cdot (dA)_n$: A_{xx} = 7.15 G; A_{yy} = 7.35 G; A_{zz} = 35.6 G; g_{xx} = 2.0088; g_{yy} = 2.0059; g_{zz} = 2.0026; T_2^{-1} = 0.8 G for all above except $(ls^4U,U)_n \cdot (A)_n$[b] and $(DUMBT,dT)_n \cdot (dA)_n$ where T_2^{-1} = 1.0 G. Parameters for $(RUMMT,U)_n \cdot (A)_n$, $(lss^4U,U)_n \cdot (A)_n$, $(ls^4U,U)_n \cdot (A)_n$, $(DUMMT,dT)_n \cdot (dA)_n$, and $(ls^4dU,dT)_n \cdot (dA)_n$: A_{xx} = 7.35 G; A_{yy} = 35.6 G; Z_{zz} = 7.15 G; g_{xx} = 2.0059; g_{yy} = 2.0026; g_{zz} = 2.0088; T_2^{-1} = 0.4 G for $(RUMMT,U)_n \cdot (A)_n$ and $(lss^4U,U)_n \cdot (A)_n$; T_2^{-1} = 1.0 G for $(ls^4U,U)_n \cdot (A)_n$ and $(ls^4dU,dT)_n \cdot (dA)_n$; T_2^{-1} = 0.6 G for $(DUMMT,dT)_n \cdot (dA)_n$. [b] From Kao et al. (1983). [c] From Bobst et al. (1984).

values derived from ESR data.

The experimental ESR spectra of single-stranded (ls^{4}dU,-dT)$_n$ and double-stranded (ls^{4}dU,dT)$_n$·(dA)$_n$ both display narrow-lined spectra (data not shown). The parameters used for the simulation of these spectra are listed in Tables I and II. The tether length is the same in ls^{4}dU as in DUTT, and the ESR spectra of (ls^{4}dU,dT)$_n$ and (DUTT,dT)$_n$ are essentially the same as is shown with the ESR simulation parameters listed in Table I. Annealing the two spin-labeled single strands with (dA)$_n$ gives rise to different ESR line shapes for the two duplexes. (ls^{4}dU,dT)$_n$·(dA)$_n$ shows a spectrum characteristic of single strands with a $\tau_\perp$ value of 1.2 ns (Table II) found for non-base-paired spin-labeled nucleotides. This observation is not unexpected in view of the positioning of the label, which should interfere with Watson–Crick base pairing. On the other hand, the spin-label position in DUTT allows for normal base pairing, and (DUTT,dT)$_n$·(dA)$_n$ gives a $\tau_\perp$ value of 4 ns as do all pyrimidine bases spin-labeled in position 5 upon annealing with the complementary base. Note that the fast axis of reorientation (z') of the nitroxide molecular axis (x, y, z) is the same for (DUTT,dT)$_n$, (DUTT,dT)$_n$·(dA)$_n$, and (ls^{4}dU,dT)$_n$ (Tables I and II). In all these systems $z' = z$. This was found to no longer be the case for (ls^{4}dU,-dT)$_n$·(dA)$_n$, where $z' = x$ (Table II). From viewing the model shown in Figure 3 it becomes apparent that the complementary dA sterically hinders the nitroxide ring and forces it to flip around bond 2 by 90° so that z' equals x. Whether the nitroxide ring is flipped into the major or minor groove is at present not known, although we favor the minor groove as the location of the ring on the basis of results obtained with lss^{4}U (see below).

It was concluded earlier that ls^{4}U in (ls^{4}U,U)$_n$·(A)$_n$ resides in a non-base-paired configuration after comparing its narrow-lined spectrum with the considerably more broadened spectrum of (RUTT,U)$_n$·(A)$_n$ (Kao et al., 1983). The same characteristic effect caused by the positioning of the label on the pyrimidine base has now also been observed with the DNA analogue (ls^{4}dU,dT)$_n$·(dA)$_n$, further corroborating the conclusion that a spin-label in position 4 of a pyrimidine base interferes with Watson–Crick base pairing. A non-base-paired configuration could therefore also be expected with the 4-substituted lss^{4}U upon annealing of (lss^{4}U,U)$_n$ with (A)$_n$. This was indeed observed in the ESR spectrum of (lss^{4}U,U)$_n$·(A)$_n$ (data not shown), although for this system the base motion, reflected in $\tau_\perp$, increases from 1.2 to 2.8 ns. Previously, the non-base-paired spin-labeled bases in (ls^{4}U,U)$_n$·(A)$_n$ and (ls^{4}dU,dT)$_n$·(dA)$_n$ had displayed the same mobility as the spin-labeled bases in the corresponding single strands (Tables I and II). The slowing down of the motion of lss^{4}U upon annealing with (A)$_n$ is attributed to its shorter tether length as compared to that in ls^{4}U. The shorter tether will put the nitroxide ring in close proximity with the sugar backbone of the minor groove, which should to some extent cause a steric hindrance of the base motion. As for ls^{4}U, the annealing process could flip the nitroxide ring around bond 2 (see Figure 3) by 90° into the major or minor groove so that z' equals x. The evidence that the nitroxide ring resides in the minor groove as shown in Figure 5 is based on the $\tau_\parallel$ value, which is smaller for (lss^{4}U,U)$_n$·(A)$_n$ than for (RUMMT,U)$_n$·(A)$_n$, thereby reflecting the small depth of the minor groove vs. the major groove in A RNA. The same argument can also be used for explaining the difference in $\tau_\parallel$ between (ls^{4}U,U)$_n$·(A)$_n$ and (RUTT,U)$_n$·(A)$_n$.

We pointed out earlier that the simulation solutions are not unique if we consider each system separately (Kao et al., 1983).

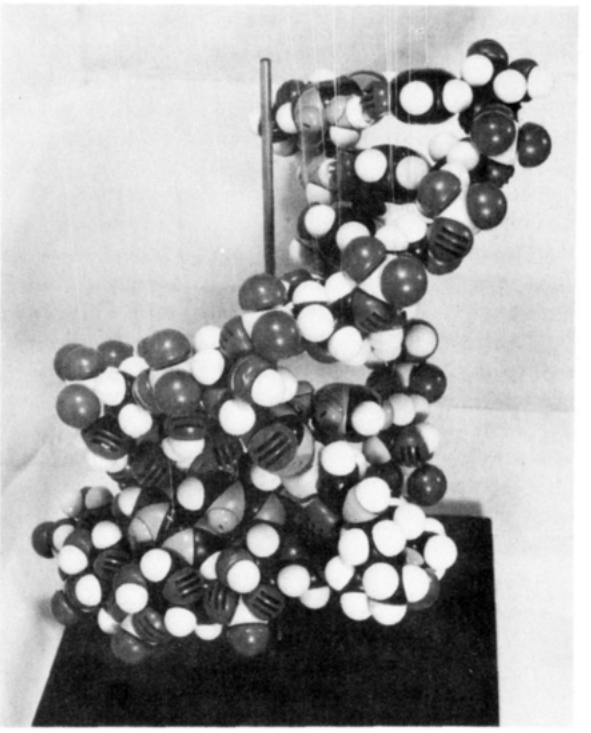

FIGURE 5: CPK model of (lss^{4}U,U)$_n$·(A)$_n$ in the A-form RNA with atomic coordinates from Arnott et al. (1969). On the right lower part of the figure one sees the probe attached to a U base in position 4. The substituted U is non base paired with A and protrudes into the minor groove.

This should be reemphasized, especially in view of the two solutions given for (ls^{4}U,U)$_n$·(A)$_n$ (Table II). In the case of (ls^{4}U,U)$_n$·(A)$_n$, the solution for the non-base-paired duplex was founded on one single case (Kao et al., 1983), whereas the more recent solution involving a permutation of $z' = z$ to $z' = x$ allows us to simulate with the same model the additional non-base-paired systems (lss^{4}U,U)$_n$·(A)$_n$ and (ls^{4}dU,dT)$_n$·(dA)$_n$.

In Table I and II we also list he line-broadening term T_2^{-1}, whose definition was given under Materials and Methods. T_2^{-1} was found to be 1.2 G for all spin-labeled single-stranded systems except for those containing the shortest tether as found in RUMMT, DUMMT, and lss^{4}U. These latter systems required a value of 0.8 G for T_2^{-1}, and the reduction in their T_2^{-1} is attributed to the presence of an additional hydroxyl group in the nitroxide ring. The annealing of the spin-labeled nucleic acids with the complementary strands results in an overall reduction of the T_2^{-1} values for all systems. The absolute value of T_2^{-1} gets smaller the deeper the probe is buried in the duplex and increases in value the more the probe is removed from the helical axis. It could be hypothesized that T_2^{-1} depends in part also on the water accessibility of the nitroxide, which presumably is the largest when it is furthest removed from the helical axis.

The tilt angle, which is defined as the angle between the principal rotational diffusion axis z' and the molecular hyperfine principal z axis (Bobst et al., 1984) (see Figure 3), is also given in Tables I and II. The angle is of the order of 55 ± 5° for all single strands except for (RUMMT,U)$_n$, (lss^{4}U,U)$_n$, and (DUMMT,dT)$_n$ whose angles are slightly smaller with a value of 45° ± 5°. This difference is believed to be caused by the presence of a hydroxyl group in the nitroxide ring of RUMMT, lss^{4}U, and DUMMT. Base pairing causes only a small reduction of the angle in all those systems where the probe should experience little if any steric hindrance.

No change in angle is obtained for $(DUMBT,dT)_n \cdot (dA)_n$ in which the probe sticks out of the major groove. A considerably larger change in the angle was required for the probes with the shortest leg as a result of base pairing, which should again reflect steric interference between probe and lattice.

The motional model also allows us to distinguish between RNA and DNA duplexes (Table II), whereas the line shapes and parameters of the single-stranded RNA and DNA systems are essentially undistinguishable (Table I). From Table II it is apparent that $\tau_{\parallel}$ for a given tether size is shorter by a factor of 2 or more for DNA than for RNA duplexes. For the 5-substituted derivatives, where the probe resides in the major groove, the larger $\tau_{\parallel}$ values observed in the RNA duplexes reflect the greater depth of its major groove as compared to that present in B-form-like DNA duplexes. Namely, B-form-like DNA contains a major groove with a depth of the order of 8 Å as determined by X-ray fiber studies (Arnott, 1981), a value that agrees with our recent solution measurements (Bobst et al., 1984). On the other hand, the major groove in an RNA duplex as shown in Figure 5 is about 13 Å deep (Arnott, 1981).

In summary, we show for a number of spin-labeled RNA and DNA single- and double-stranded systems the existence of substantial base motion on the nanosecond time scale. The conclusion is based on a simple motional model that not only gives information about the base dynamics but also allows us to draw conclusions about some of the structural features of the systems. The number of spin-labeled nucleic acids that fit the model has been increased to 22, and they can all be analyzed with the same motional model, which suggests its general applicability for the analysis of ESR spectra of spin-labeled nucleic acids.

Registry No. ppRUMMT, 87373-18-0; ppRUTT, 87373-19-1; ppRUMPT, 87373-20-4; ppls^{4}U, 87373-21-5; pplss^{4}U, 97721-13-6; pppDUMBT, 89900-69-6; pppDUMMT, 89900-67-4; pppDUTT, 82187-53-9; pppDUMPT, 82187-55-1; pppDUAT, 97721-14-7; pppls^{4}dU, 97721-15-8; $(RUMMT,U)_n$, 87373-24-8; $(RUTT,U)_n$, 87373-26-0; $(RUMPT,U)_n$, 87373-28-2; $(lss^4U,U)_n$, 97721-05-6; $(ls_4U,U)_n$, 87373-30-6; $(DUMMT,dT)_n$, 89883-52-3; $(DUTT,dT)_n$, 89883-54-5; $(DUMPT,dT)_n$, 89883-57-8; $(DUAT,dT)_n$, 97721-07-8; $(DUMBT,dT)_n$, 89883-60-3; $(ls^4dU,dT)_n$, 97721-09-0; $(RUMMT,U)_n \cdot (A)_n$, 87373-32-8; $(RUTT,U)_n \cdot (A)_n$, 87373-34-0; $(RUMPT,U)_n \cdot (A)_n$, 87373-36-2; $(lss^4U,U)_n \cdot (A)_n$, 97721-10-3; $(ls^4U,U)_n \cdot (A)_n$, 87373-37-3; $(DUMMT,dT)_n \cdot (dA)_n$, 89883-53-4; $(DUTT,dT)_n \cdot (dA)_n$, 89883-55-6; $(DUMPT,dT)_n \cdot (dA)_n$, 89883-58-9; $(DUAT,dT)_n \cdot (dA)_n$, 97721-11-4; $(DUMBT,dT)_n \cdot (dA)_n$, 89889-02-1; $(ls^4dU,dT)_n \cdot (dA)_n$, 97721-12-5; uridine 5′-diphosphate, 58-98-0; thymidine 5′-triphosphate, 365-08-2.

References

Allison, S. A., Shibata, J. H., Wilcoxon, J., & Schurr, J. M. (1982) *Biopolymers 21*, 729–762.

Arnott, S. (1981) in *Topics in Nucleic Acid Structure* (Neidle, S., Ed.) pp 65–82, Wiley, New York.

Arnott, S., Dover, S. D., & Wonacott, A. J. (1969) *Acta Crystallogr., Sect. B.: Struct. Crystallogr. Cryst. Chem. B25*, 2192–2206.

Assa-Munt, N., Granot, J., Behling, R. W., & Kearns, D. R. (1984) *Biochemistry 23*, 944–955.

Barkley, M. D., & Zimm, B. H. (1979) *J. Chem. Phys. 70*, 2991–3007.

Bobst, A. M. (1971) *Macromolecular Preprint, International Congress of Pure and Applied Chemistry, 23rd*, Boston, 1971, Pergamon Press, New York.

Bobst, A. M. (1972) *Biopolymers 11*, 1421–1433.

Bobst, A. M. (1980) in *Molecular Motion in Polymers by ESR* (Boyer, R. F., & Keinath, S. E., Eds.) pp 167–175, Harwood, New York.

Bobst, A. M., Ireland, J. C., & Langemeier, P. W. (1981) *Biophys. J. 33*, 313a.

Bobst, A. M., Kao, S.-C., Toppin, R. C., Ireland, J. C., & Thomas, I. E. (1984) *J. Mol. Biol. 173*, 63–74.

Bolton, P. H., & James, T. L. (1979) *J. Phys. Chem. 83*, 3359–3366.

Early, T. A., & Kearns, D. R. (1979) *Proc. Natl. Acad. Sci. U.S.A. 76*, 4165–4169.

Freed, J. H. (1976) in *Spin Labeling: Theory and Applications* (Berliner, L. J., Ed.) pp 53–132, Academic Press, New York.

Hakam, A., Thomas, I. E., & Bobst, A. M. (1980) *Int. J. Biol. Macromol. 2*, 49–51.

Hogan, M. E., & Jardetzky, O. (1979) *Proc. Natl. Acad. Sci. U.S.A. 76*, 6341–6345.

Hurley, I., Osei-Gyimah, P., Archer, S., Scholes, C. P., & Lerman, L. S. (1982) *Biochemistry 21*, 4999–5009.

Ireland, J. C., Willett, J. A., & Bobst, A. M. (1983) *J. Biochem. Biophys. Methods 8*, 49–56.

Kao, S.-C., Polnaszek, C. F., Toppin, C. R., & Bobst, A. M. (1983) *Biochemistry 22*, 5563–5568.

Keepers, J. W., & James, T. L. (1982) *J. Am. Chem. Soc. 104*, 929–939.

Klevan, L., Armitage, I. M., & Crothers, D. M. (1979) *Nucleic Acids Res. 6*, 1607–1616.

Langemeier, P. W., & Bobst, A. M. (1981) *Arch. Biochem. Biophys. 208*, 205–211.

Pan, Y.-C., & Bobst, A. M. (1973) *Biopolymers 12*, 367–371.

Polnaszek, C. F. (1976) Ph.D. Thesis, Cornell University, Ithaca, NY.

Robinson, B. H., Forgacs, G., Dalton, L. R., & Frisch, H. L. (1980a) *J. Chem. Phys. 73*, 4688–4692.

Robinson, B. H., Lerman, L. S., Beth, A. H., Frisch, H. L., Dalton, L. R., & Auer, C. (1980b) *J. Mol. Biol. 139*, 19–44.

Saenger, W. (1984) in *Principles of Nucleic Acid Structure*, Springer-Verlag, New York.

Toppin, C. R., Thomas, I. E., Bobst, E. V., & Bobst, A. M. (1983) *Int. J. Biol. Macromol. 5*, 33–36.

Toppin, C. R., Pauly, G., Devanesan, P., & Bobst, A. M. (1985) *Helv. Chim. Acta* (submitted for publication).

Wang, J., Hogan, M. E., & Austin, R. H. (1982) *Proc. Natl. Acad. Sci. U.S.A. 79*, 5896–5900.

Warwick, P. E., Hakam, A., Bobst, E. V., & Bobst, A. M. (1980) *Proc. Natl. Acad. Sci. U.S.A. 77*, 4574–4577.